

STUDY OF RELATIONSHIP BETWEEN THE PRESENT-DAY REGIONAL STRESS FIELD WITH FAULT'S GEOMETRIC PARAMETERS DETERMINING THE RELATIVE DISPLACEMENT OF THE EARTH'S CRUST IN THE SOUTH CHINA SEA AND ADJACENT AREAS

Tran Tuan Dung¹, Bui Cong Que², Nguyen Quang Minh¹

¹*Institute of Marine Geology and Geophysics, Vietnam Academy of Science and Technology, 18 Hoang Quoc Viet, Cau Giay, Hanoi, Vietnam; e-mail: trantuandung@yahoo.com*

²*Institute of Marine Geology and Geophysics, VAST, Building A27, 18 Hoang Quoc Viet, Cau Giay, Hanoi, Vietnam; e-mail: qminh@imgg.vast.vn*

Поступила в редакцию 22 апреля 2016 г.

In this paper, the present-day regional stress field in the South China Sea is determined through the earthquake's focal mechanism parameters that have recorded more than 100 years. The geometric parameters of the faults (such as the location, dip angle, strike angle as well as depth, length and horizontal destructive zone) are determined by gravity, seismic data and regional stress fields.

Here, predictive study of the magnitude and tendency of the relative displacement of the Earth's crust are carried out by calculating and assessing the relationship between the regional stress fields with fault geometric parameters. On the basis of the Earth's crust relative displacement, the geodynamics mechanism can be rebuilt through different geological periods in the South China Sea and adjacent areas.

Magnitude and tendency of the relative displacement of the Earth's crust are represented by the color spectrum and the vector's magnitude. Although the displacement appears in the whole of the region, they have different intensity in particular areas with different grade fault systems.

Keywords: South China Sea, faults, present-day regional stress field, Earth's crust displacement.

INTRODUCTION

In general, in tectonic research, each area in the world has a stress field with different parameters, respectively. Their changes over time depend on the interaction of the tectonic plates in the Earth's crust. Stress field plays a very important role in formation and activities of new fault systems which cause the displacement of the Earth's crust. Therefore, based on the relationship between the regional stress field with fault geometric parameters, the tendency of active fault as well as predict the risk of landslide, and earthquake can be evaluated.

The theory on fault slip was first mentioned by Bott M.H.P (1959) [3]. It is proved that the fault slip vector is parallel with the shear stress on the fault plane. According to this hypothesis, they have identified the sliding activity of fault in a specific stress field. After that, the hypothesis, is widely known under the name of Wallace-Bott and is used as a method of the inversion stress field.

This hypothesis was further studied and developed by McKenzie (1969) [8]. This study has shown that the

evidence of earthquakes occur almost on the existent fault. Since then, the idea of using data of Earthquake's focal mechanism (EFM) determining the existent fault behavior is widely used.

The above-mentioned hypothesis is continuously developed to determine the fault reactive by Angelier J. et al. (1990); Morris A. et al. (1996) [2], [9]. In particular, they have pointed out that the slip vector of fault depends not only on the principal stress axes, but also on the stress ratio $\phi = (\sigma_2 - \sigma_3) / (\sigma_1 - \sigma_3)$. Here, the slip tendency is determined by the ratio of shear stress and normal stress on a fault plane. This is an important major premise for the next researches on active or reactivated faults (Neves M.C. et al., 2009; Tong H-M. et al., 2011; McFarland J.M. et al., 2012; Yukutake Y. et al., 2015), [8], [7], [14], [18]. These studies have shown the suitability of the methods in fault's activity. However, in these researches, the effects of fault displacement on the Earth's crust has not been mentioned. In 1980, Aki K. and Richards P.G., [1] have

proposed the conventions on fault parameters, which are strike, dip and rake, based on EFM data. From now on, this study will follow this conventions to determine and display the fault parameters.

Nguyen Van Vuong et al. (2004) have determined the nature of Earth’s crust intraplate deformation and present-day displacement, which occur along the fault system in the North Western of Vietnam, under the impact of regional stress field and the related earthquakes. The results have revealed the characteristics on stress change and the relative displacement of the structural blocks. The location of the earthquake’s epicentre also was predicted along main faults in the area [10]. In 2015, Tran Tuan Dung et al., have also determined the horizontal and vertical displacement of the Earth’s crust that are based on the relationship between the regional stress field with faults geometric parameters. On these results, the author has evaluated and zoned the submarine landslide potential in Phu Khanh Basin and adjacent areas [15].

The study area is located on the Eurasian plate, the EFM’s of many intraplate earthquakes are recorded and covered in the whole area. In this study, the regional stress field is calculated by the dataset of EFM’s that have recorded more than 100 years so far. In this study, the geometric parameters of faults (such as spatial position, strike, dip) were determined by gravity and seismic meth-

ods. Subsequently, the geometry-dynamic parameters of the fault systems (such as slip vector, slip tendency) are identified by using regional stress field. On these basis, the relative displacement tendency in horizontal and vertical direction of the Earth’s crust will be calculated.

DATA USED

Earthquake’s focal mechanisms data

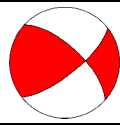
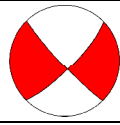
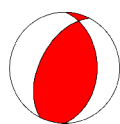
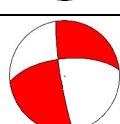
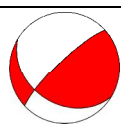
The earthquake’s focal mechanisms (EFM) dataset are recorded from many different sources, in these, primarily from the Global Centroid-Moment-Tensor Project in primarily (120 earthquakes) [5] and from the study of Bui Cong Que et al., (19 earthquakes) [4]. The focal mechanisms of intraplate earthquakes were collected at depth ≥ 5 km and magnitude ≥ 3.0 (Figure 1).

This study uses 139 EFM’s that are available in the study area. However, in the framework of an article, only some samples of EFM’s are shown in Table 1.

Seismic data

In recent years, the marine survey projects of Vietnam together with the international cooperation have added more information on geology and geophysics with more detail and high accuracy, especially seismic exploration. In this study, only the interpreted results from the previous projects are used, as follows: AW-HS; PK-3; PGS-8, 9; WA-74; NOPEC-93; VOR-93; SEAS-

Table 1. Some samples of the earthquake’s focal mechanism dataset [4], [5].

No	Date	Lat.	Long.	Depth	M _w	Strike	Dip	Rake	S _{Hmax}	Stress Regime	Focal mechanism
1	1905/7/13	19.9	110.5	-	7.5	313	66	160	2	SS	
3	1969/12/17	18.11	110.55	33	4.7	45	78	-6	0	SS	
4	1977/8/29	17.38	119.61	24.6	6.3	1	41	70	104	TF	
5	1995/1/10	20.57	109.33	15	5.5	264	64	-173	127	SS	
...
139	2015/11/7	16.64	119.8	61.5	5.4	121	35	161	174	SS	

Where: Depth (km); M_w – moment magnitude; S_{Hmax} – Maximum horizontal stress axis; SS – Strike slip; NF – Normal fault; TF: Thust fault.

95; SEAS-TC; TC-93, 95, 98; TC-03, 6; VGP-09-08, PV, STC-6; CPV-05, 07; PKBE-07, 08; JMSU-05, 07. These valuable seismic data sources are used in combination with gravity data to identify correctly the geometric parameters of faults (Fig. 1) [4], [15], [16].

Gravity data

The gravity data in the South China Sea and adjacent areas have been mainly collected from the joint shipboard surveys between Vietnam and foreign countries, such as Russia, America, France, Germany and Japan... Also there are a lot of national projects, which are carried

out by Institute of Marine Geology and Geophysics and others. These projects have completed and brought out the new useful results, and gravity anomaly maps with scale of 1:500.000, 1:250.000 are constructed for the whole region as well [16], [17].

Besides, in marine investigation, satellite altimetry is the only way to achieve the data with a uniform resolution and in acceptable time and cost, especially for remote and sensitive conflict regions. Typically, Sandwell, D.T. and W.H.F. Smith have used the satellite altimeter data to produce a satellite altimetry-derived gravity grid with interval of 1'x1' (V23.1) for most of the ocean all over the world [12].

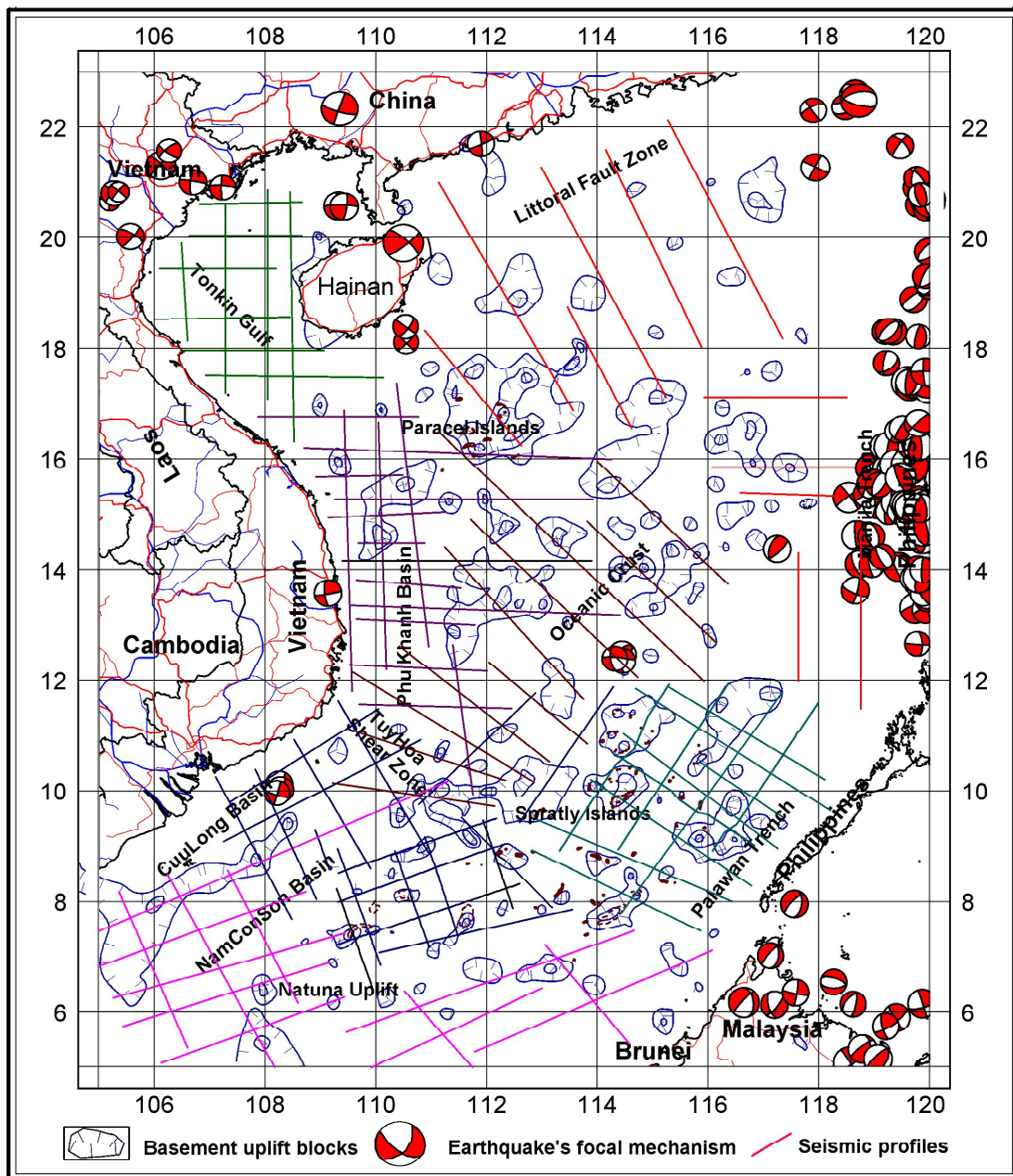


Fig. 1. Earthquake's focal mechanisms and seismic pro files.

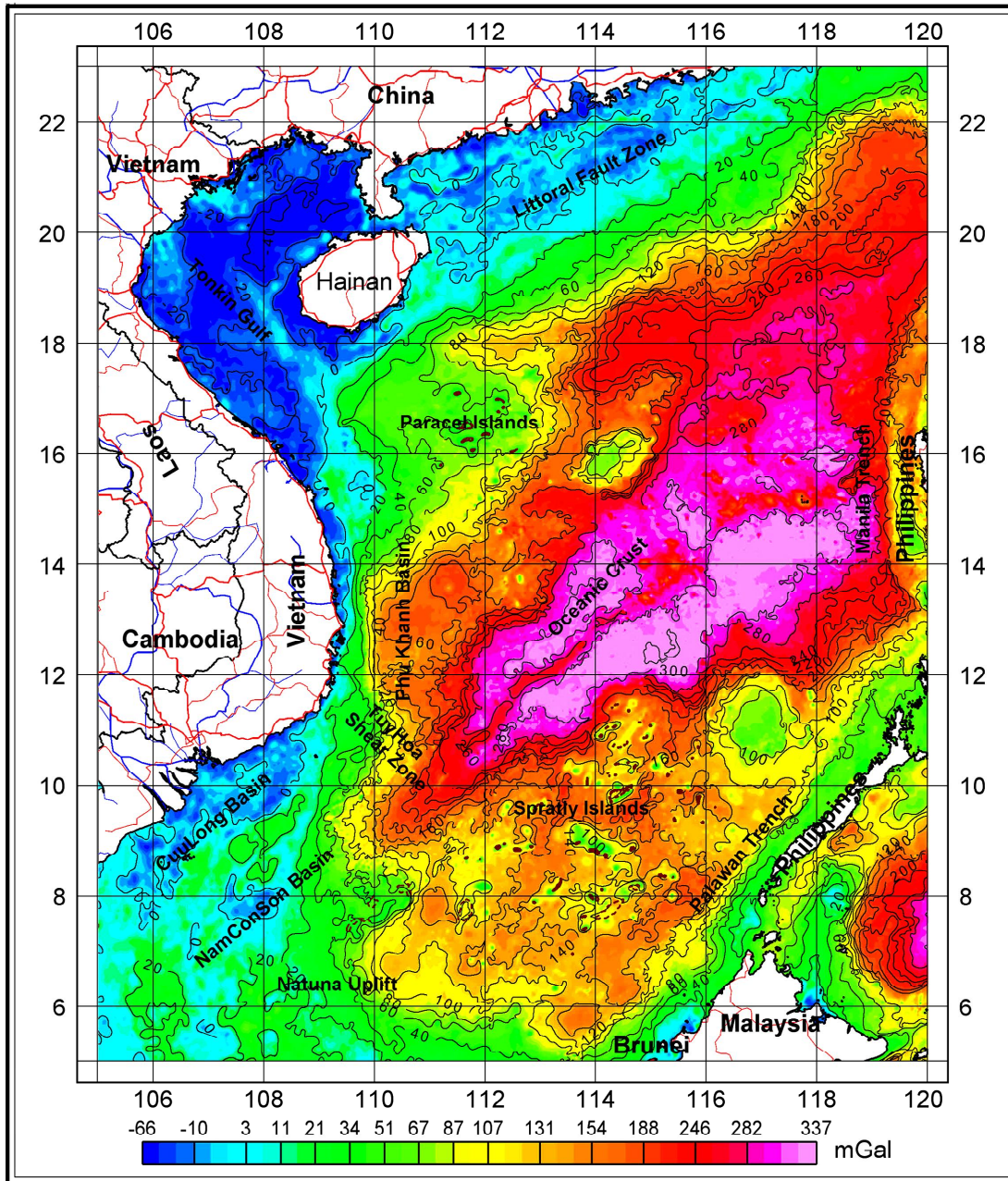


Fig. 2. Bouguer gravity anomaly.

In this study, the authors have used the satellite-shipboard-derived data, which is a successful combination of satellite altimetry-derived gravity and shipboard gravity data, with a high accuracy and uniform resolution in the South China Sea (Fig. 2) [12], [16], [17].

METHODS APPLIED

Research and determination of fault geometric parameters (spatial location, dip angle, net slip, rake) in the South China Sea is a complicated problem that cannot be solved only by a single method. The researches

must have an overall view on relationship between present-day regional stress and fault systems. Based on that relationship, the tendency and magnitude of relative horizontal and vertical displacement of the Earth’s crust can be determined. With this purpose, this paper presents some methods as follows:

Determination of the fault geometric parameters by gravity data

To determine the fault geometric parameters by gravity data, the authors used two methods, as follows:

Frequency filtering of gravity field

In general, the high frequency component of the gravity field with short wavelength associates to geological bodies at a shallow depth. On the contrary, the low frequency component of the gravity field with long wavelength reflects geological structure at a greater depth. The authors have applied the frequency filtering method, which is presented by Tran Tuan Dung et al. (2016) [17], to separate the gravity effect of the layers at different depth from the Bouguer gravity anomaly.

Low-pass filter of gravity anomalies are calculated by the following formula [17]:

$$F\{\Delta g_{LF}(x, y)\} = F\{H(x, y)\}F\{\Delta g(x, y)\} \quad (1)$$

Where: $F\{\}$ is Fourier transform; $\Delta g_{LF}(x, y)$ is low frequency anomalies that filtered with $H(x, y)$ operator; $\Delta g(x, y)$ is complete Bouguer gravity anomaly; $H(x, y)$ is the low-pass filter operator.

The Gaussian low-pass filter operator as follows:

$$H(x, y) = e^{-D(x, y)^2 / 2\lambda^2} \quad (2)$$

Where: $D(x, y)$ is the distance between point (x, y) on the grid and the center point of filtering window; λ is cutoff wavelength.

After doing low-pass filter with different wavelength λ , the gravity anomalies that correspond to these wavelengths will be used to determine the fault characters at different depths.

Horizontal gradient and maximum horizontal gradient of gravity anomalies

The maximum gravity horizontal gradient (MGHG) manifests clearly the rock density boundaries, of course, with a certain point of view, it can be said that they are the faults. The faults are often displayed by bands of the MGHG vectors that the same directions. The rock blocks, which have the density higher than that at the surroundings, are shown by the maximum gravity horizontal gradient vectors inward to the center of the blocks [16].

In this paper, the authors have used the method, which is presented by Tran Tuan Dung et al. 2016 [16], the locations and magnitudes of the MGHG $H[\Delta g]_{i,j}$ are defined by a second-order polynomial as follows:

$$X_{Max} = \frac{bd}{2a}; \quad (3)$$

$$G_{Max} = aX_{Max}^2 + bX_{Max} + H[\Delta g]_{i,j} \quad (4)$$

Here, d is the distance between grid intersections, a , b are developed coefficient of the polynomial, which are calculated from the grid of the gravity anomalies.

By analyzing and linking the locations and magnitudes of the maximum gravity horizontal gradient

by suitable methods, a general picture on fault's spatial locations at different depth have been presented.

Determination of present-day regional stress field and slip tendency of faults

Determining the regional stress field

The present-day regional stress field is characterized by the earthquake's focal mechanism in the region and adjacent area (Table 1). Based on similarities in terms of maximum horizontal stress axis, the study area will be divided into separate zones, in which the EFMs are homogeneous. Subsequently, the right dihedral method which was presented by Angelier J. (1990) [2] will be applied to determine the direction of the principal stress axes (compression, intermediate and extension) based on the EFMs of each zone, respectively.

In fact, especially for marine research, the magnitudes of principal stress ($\sigma_1, \sigma_2, \sigma_3$) are very difficult to determine. Therefore, in 1990, Angelier J., presented a quantity called the different stress ratio (ϕ), which does not depend on the magnitudes of principal stress [2].

Different stress ratio (ϕ) is determined based on the studies of Angelier J., (1990) [2]:

$$\phi = \frac{(\sigma_2 - \sigma_3)}{(\sigma_1 - \sigma_3)} \quad (5)$$

Where: $\sigma_1, \sigma_2, \sigma_3$ are magnitudes of the principal stresses and satisfying $\sigma_1 \leq \sigma_2 \leq \sigma_3$.

When obtained ratio ϕ and direction of principal stress axes ($\vec{\sigma}_1, \vec{\sigma}_2, \vec{\sigma}_3$), can be determined the shear stress (σ_s) and normal stress (σ_n) on the fault plane.

Determining the slip tendency and slip vector on fault's plane

The slip tendency on fault according to the regional stress field is defined as the ratio between the shear stress and normal stress on fault's plane. The slip vector on fault's plane is assumed to be parallel with the shear stress [9], [18]. This study follows this assumption. The slip tendency is used to determine the relative displacement of faults in the area. Slip tendency (T_s) is presented by Yukutake Y. et al., (2015) [18]:

$$T_s = \frac{|\sigma_s|}{\mu|\sigma_n|} \quad (6)$$

Where: σ_s and σ_n are the shear stress and normal stress, respectively; μ is the coefficient of friction on fault's plane, μ is chosen as 0.65 (Schellart W.P., 2000) [19]. In this study, the shear stress and normal stress on fault plane are determined based on the present-day regional stress field.

Because the coefficient of friction is put into the formula above, the more tendency values increasing the more magnitude of shear stress approaching to the frictional force. A fault with a higher value of slip tendency is more unstable in the relationship with regional stress field.

Determination of relative displacement of the Earth’s crust

The basic theory on displacement characteristics of the Earth’s crust, which is impacted by the present-day regional stress field and fault activities, was presented in study of Okada Y., (1992) [11], in which he proposed a new approach in determining displacement field in a half-space, which is based on the method introduced by Steketee J. A., (1958) [20].

Accordingly, the displacement field $u_i(x_1, x_2, x_3)$ caused by a dislocation $\Delta u_j(\xi_1, \xi_2, \xi_3)$ across a surface in an isotropic space, is represented by the formula [11], [20]:

$$u_i = \frac{1}{F} \iint_{\Sigma} \Delta u_j \left[\lambda \delta_{jk} \frac{\partial u_i^n}{\partial \xi_n} + \mu \left(\frac{\partial u_i^j}{\partial \xi_k} + \frac{\partial u_i^k}{\partial \xi_j} \right) \right] v_k d\Sigma \quad (7)$$

Where: v_k is the direction cosine of the normal to the surface element $d\Sigma$, i.e., $(0, -\sin\delta, \cos\delta)$.

Based on the formula (7) and body force equivalent relations, the internal displacement field (u^0) caused by each point source can be represented by joined forces of the strain nuclei $(\partial u^i / \partial \xi_k)$. The point source causing the fields displacement can be divided into major four categories (Fig. 3).

The displacement field on the formula (7) is developed by Toda S. et al., and integrated in the Coulomb’s open software [14]. In this study, the displacement field is a relative quantity, dimensionless,

the value of relative horizontal and vertical displacement are assigned from 0 to 1 and -1 to 1, respectively. In vertical relative displacement case, when the value changes from -1 to 0, the displacement tendency is down; on the contrary, from 0 to 1 then displacement tendency is up.

RESULTS AND DISCUSSIONS

Fault systems

With respect to the study of faults, which is based on gravity data, then the spatial distributions of the maximum gravity horizontal gradient (MGHG) are also the distributions of fault systems and rock density boundaries. The fault systems are displayed by bands of the MGHG vectors [16]. In this study, the Bouguer gravity anomalies that have filtered at wavelength $\lambda = 25, 50, 75\text{km}$ and 100 km (Figure 4) are used to calculate the horizontal gradient and the MGHG, respectively. Here, why above-mentioned wavelengths are selected, simply, for the purpose of getting a general picture on spatial distribution of the faults systems at different depths.

As usual, the spatial parameters of the faults (depth, strike, dip) are determined based on the distribution of the MGHG at different depths (Fig. 4). By analyzing and linking the locations and magnitudes of the MGHG by suitable methods, the spatial distribution of fault systems has been generated in combination with the seismic interpreted results (Fig. 5). The fault systems are mainly used inherently from previous studies of the authors in [16] (Fig.). For that reason, it is not concentrated to describe their characteristics in details.

Present-day regional stress field

Present-day regional stress field is calculated based on the earthquake’s focal mechanisms and associated

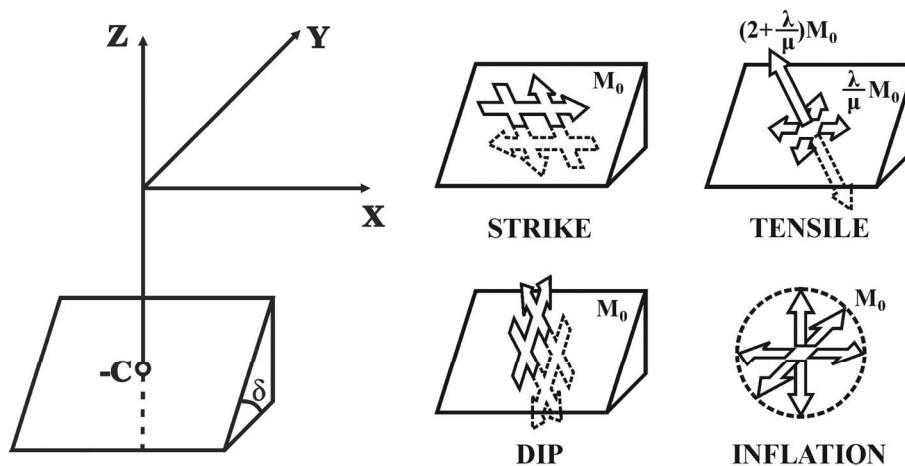


Fig. 3. Four major sources causing the displacement fields.

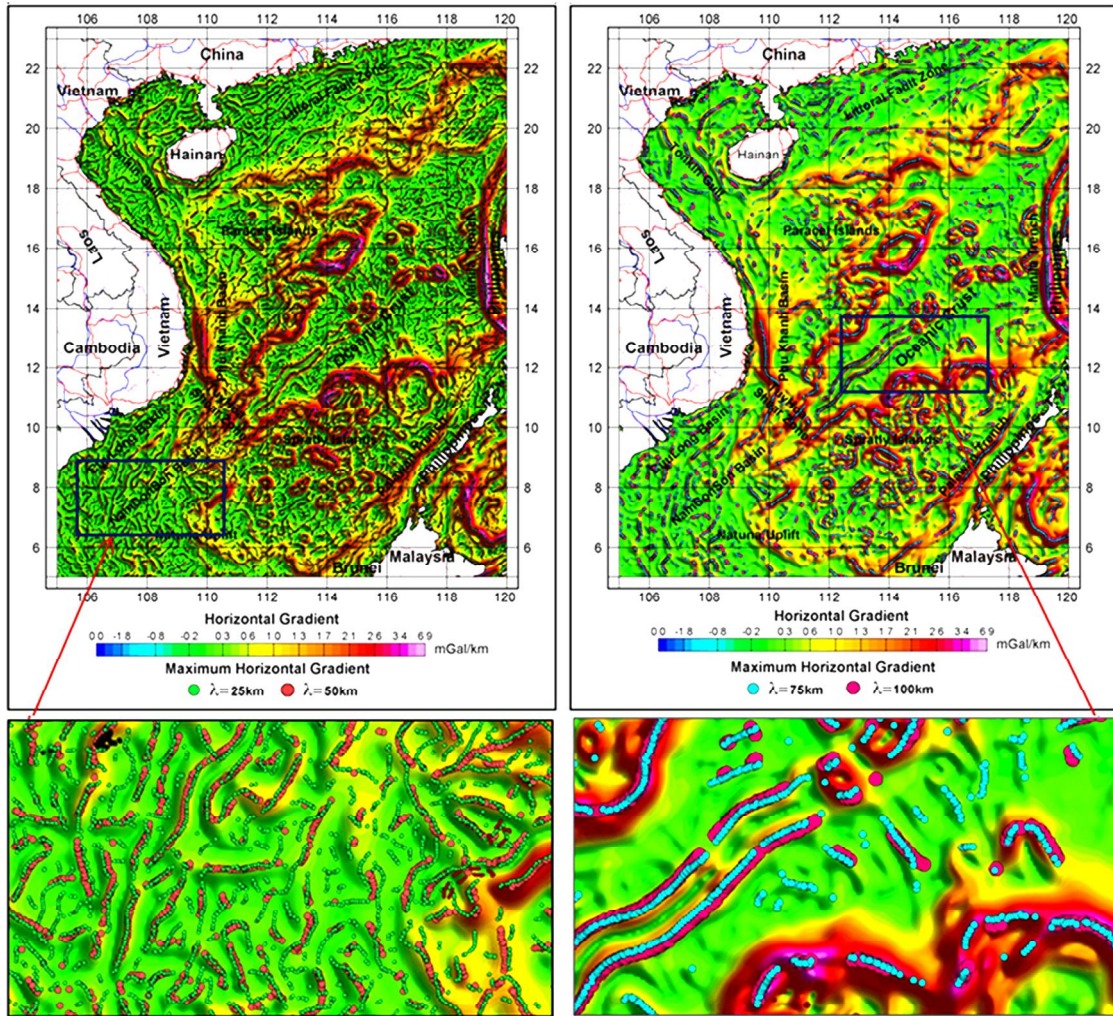


Fig. 4. Horizontal gradient and maximum horizontal gradient of gravity anomalies (filtered at wavelength $\lambda = 25, 50, 75, 100$ km).

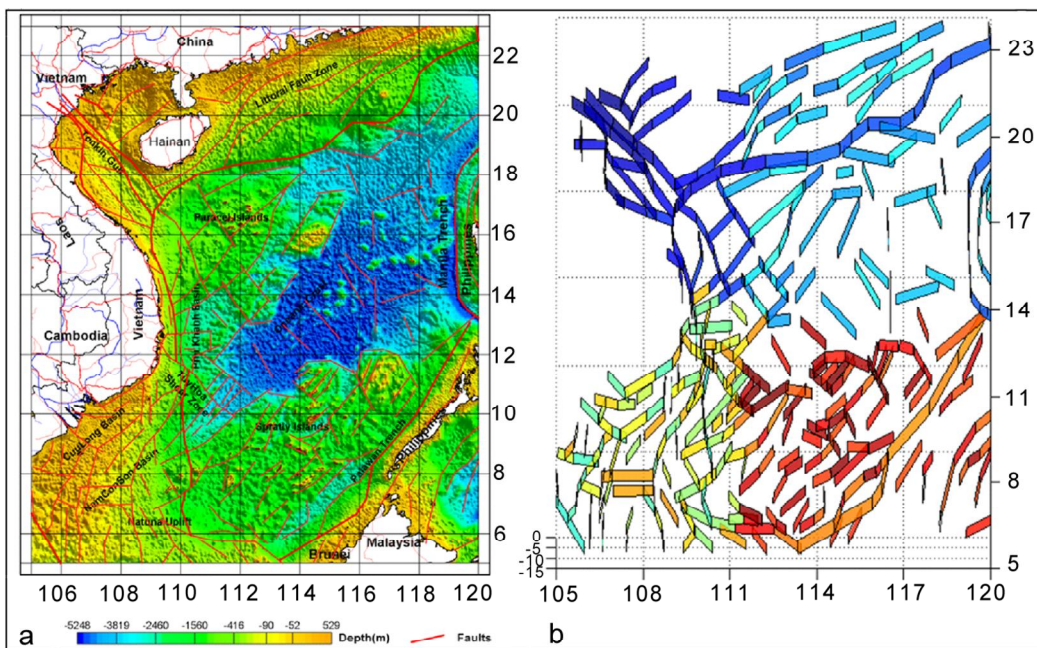


Fig. 5. Distribution of faults systems: $a > 2D$ faults; $b > 3D$ fault's parameters.

movement orientation of the Eurasian plate (Fig. 6). In the Northwest of the study area, the direction of maximal horizontal stress (MHS) axis is sub-meridian, while in the Northeast its direction is sub-parallel. From the southwest to southeast of the study areas, the direction of MHS stress axis changes from NWN-SES to NW-SE, respectively.

Based on the differences in direction of the MHS axis and EFMs, the study area is divided into five zones in order to define the parameters of present-day stress

field (Table 2). Subsequently, the behavior of the faults systems in each zone is calculated and assessed.

The fault systems on Figure 5 will be divided into five groups with respect to the stress field of the five zones, consist of 368 fault segments, respectively. Figure 7 illustrates how to split faults to segments and calculate their parameters. The sample is a graben with two faults. The fault segments are splitted based on the criteria as follows: strike and dip of each fault's segment are almost unchanged. Since then, parameters of each

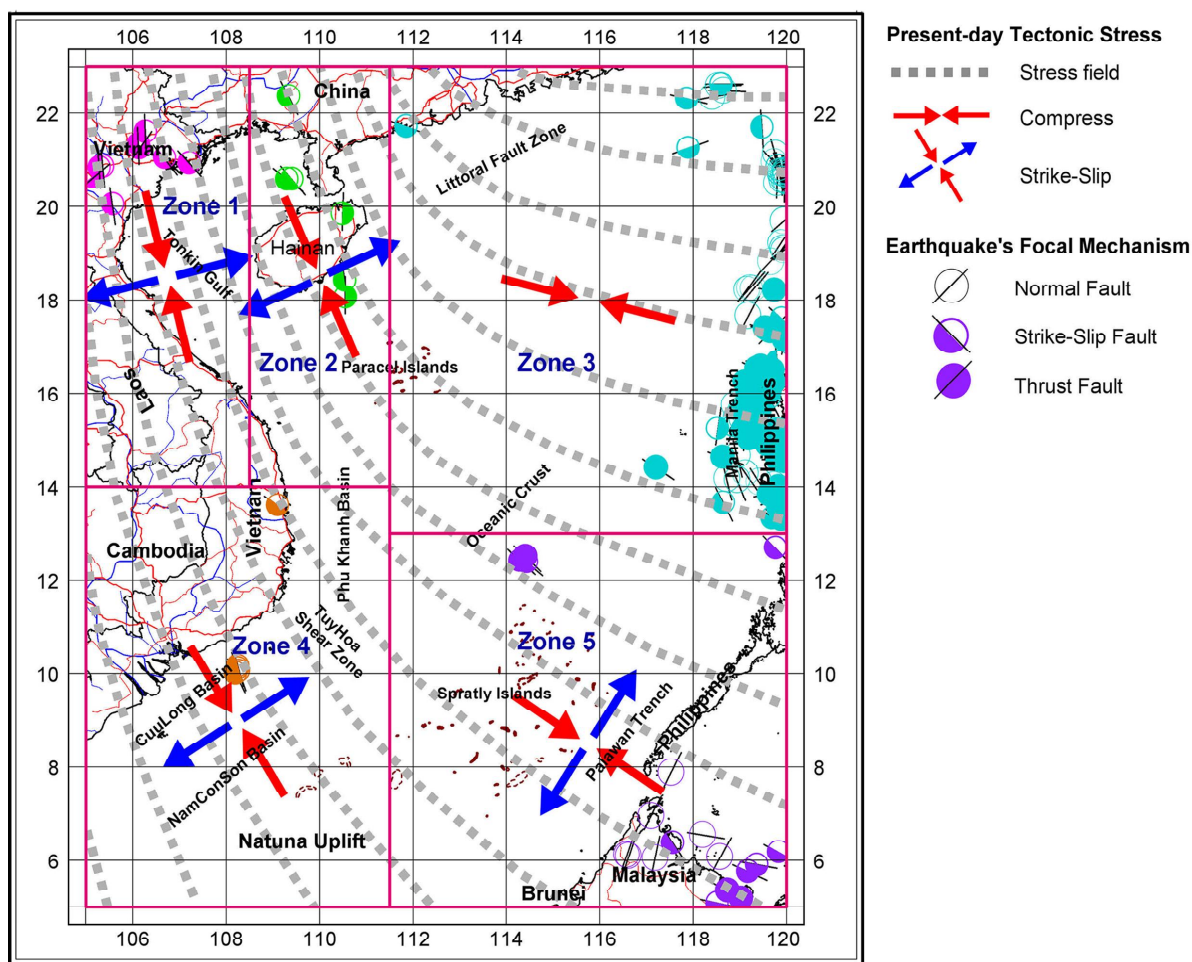


Figure 6. Present-day regional stress field.

Table 2. Result of stress inversion in each zone (see Figure 6).

Zone No	Data	σ_1		σ_2		σ_3		ϕ	S_{Hmax}
		Trend	Plunge	Trend	Plunge	Trend	Plunge		
1	9	166	11	329	78	075	03	0.33	166
2	6	154	07	046	67	247	21	0.67	156
3	101	286	21	018	06	124	69	0.45	104
4	5	148	03	260	81	058	08	0.80	148
5	18	304	07	051	67	211	22	0.23	123

fault segments are identified. The dip (δ) of fault segment is calculated as follow:

$$\delta = \arctan \frac{|FG|}{|CD|} \quad \text{Satisfying } 0 \leq \delta \leq 90^\circ$$

The slip tendency and slip vector of these fault segments are determined based on the stress field of each zone. In this paper, these of all 368 fault segments have been calculated. However, in the framework of the article, only some samples of the results are shown in Table 3.

Tendency and magnitude of relative displacement field of the Earth's crust

The present-day displacement field of the Earth's crust is determined by the formula (7). The input data of the model are the fault parameters (Table 3), which are determined by the above-mentioned methods. According to the results of the researches at [4], [16] on faults activities, in the model, the net-slip is to be replaced by the slip tendency. The possibility and magnitude of displacement of fault segments are relative which are compared between them together. The calculated depth of the model is chosen about 10km below the sea level.

In Figures 8 and 9, the color spectrum and the length of the vector show the relative magnitude and direction of the Earth's crust displacement. Although the displacement appear in all over study area, but at near large faults their magnitude appears higher. Look at the figures, one can see that the picture of the displacement field in each particular areas.

The magnitude of relative horizontal displacement (RHD) is high along the large faults (Fig. 8). In general, they are quite high in the areas, such as Tonkin gulf, Phu Khanh basin, Tuy Hoa shear zone, Nam Con Son

basin. The fault systems, which are strongly influenced by the present-day stress field, have a highly ability of reactivation.

In Manila trench the magnitude of RHD is quite high, the direction of the vector shows the strong activity of the thrust fault systems in the present-day period. Besides, in the area of Phu Khanh basin, Tuy Hoa shear zone and Natuna uplift, the magnitude of RHD is also quite high, the direction of the vector indicate the strike-slip manifestation of faults system, they have a strong possibility of reactivation in the future.

The RHD in the Tonkin Gulf, Littoral Fault Zone, Nam Con Son Basin, Paracel Islands and Spratly Islands have average magnitudes and the direction of the vector shows the strike-slip manifestation of faults system.

In Palawan trench and deep water basin of the South China Sea, the magnitude of RHD is low. It shows that the faults systems in this area are not affected by the present-day tectonic stress field in the region.

Figure 9 illustrates tendency and magnitude of the relative vertical displacement (RVD) of the Earth's crust, it shows the local tendency up-down around the faults system. The areas that have tendency up are the Tonkin gulf, North and South Phu Khanh basin, East of Hainan Island, North of Manila trench, Paracel islands, North and South Spratly islands and Natuna uplift. In contrast, in the areas, such as South of Hainan island, South of Manila trench, Center of Phu Khanh basin, Cuu Long basin and Nam Con Son basin, North of Palawan trench and Center of Spratly Islands the tendency is down.

In the Spratly islands area, the RVD has an interleaving tendency up-down along the faults systems. The tendency down is mostly available between the uplift blocks. The magnitude and tendency up-down of

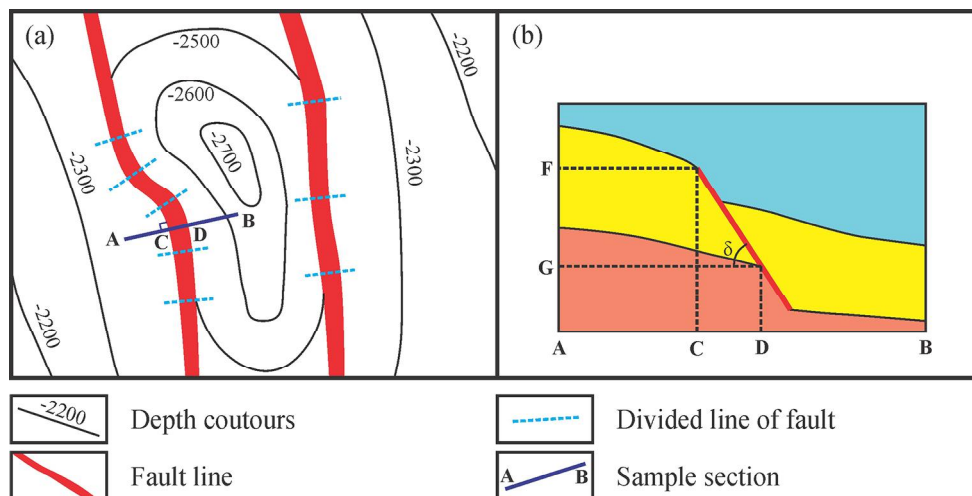


Fig. 7. Division of faults to segments and calculate its parameter.

Table 3. The geometric parameters of the fault segments that are used for calculated model.

No	Start		End		Strike	Dip	Rake	Sense of slip	Top	Bott.	T_s
	Long.	Lat.	Long.	Lat.							
Zone 1											
1	106.477	20.665	107.245	20.331	113	70	-112	RL-NR	2	8	0.13
2	106.954	19.700	107.792	18.899	134	72	-177	RL	2	8	0.41
3	106.363	19.897	105.531	20.426	302	77	84	TH	2	8	0.27
4	106.746	19.189	106.624	19.572	342	75	46	LL-TH	2.3	8.3	0.67
5	106.648	17.927	106.695	18.759	3	70	62	LL-TH	2	8	0.66
.....
Zone 2											
31	109.120	16.803	109.005	16.085	189	67	146	RL-TH	2	8	0.63
32	108.339	18.482	109.396	17.188	141	73	-121	RL-NR	2	8	0.72
33	109.629	17.453	110.694	18.080	60	65	-132	RL-NR	2.3	8.3	0.33
34	109.051	15.486	109.405	14.734	155	66	91	TH	1.5	7.5	0.65
53	109.120	16.803	109.629	17.453	38	66	-156	RL-NR	2.2	8.2	0.65
.....
Zone 3											
63	119.213	16.329	119.237	17.740	1	49	64	LL-TH	5	11	0.82
64	118.034	21.462	118.611	21.912	52	66	177	RL	3	9	0.31
65	119.999	22.544	119.934	22.999	352	70	1	LL	2.5	8.5	0.23
66	117.371	20.101	117.683	20.549	35	66	169	RL	3	9	0.18
67	115.769	19.765	116.881	19.777	89	65	171	RL	3	9	0.37
.....
Zone 4											
151	105.973	5.000	105.000	6.666	330	80	-77	NR	2.5	8.5	0.48
152	109.852	11.775	109.819	12.679	358	72	-21	LL-NR	3	9	0.93
153	109.735	13.551	109.849	12.688	172	71	-29	LL-NR	2.5	8.5	0.94
154	110.036	10.347	110.289	11.488	13	74	-9	LL	3.4	9.4	0.79
155	110.364	8.159	110.127	9.132	346	68	-42	LL-NR	4	10	0.90
.....
Zone 5											
269	118.875	11.710	119.709	13.051	32	53	79	TH	3	9	0.45
270	116.440	8.305	117.866	9.918	41	55	101	TH	3	9	0.41
271	115.893	6.642	116.223	7.157	33	52	81	TH	3	9	0.46
272	117.866	9.918	118.875	11.710	29	54	72	TH	3	9	0.45
.....
368	113.025	10.860	111.741	9.958	235	70	-43	LL-NR	5.5	10.5	0.60

Where: Start, End: start and end position of fault; Strike, Dip, Rake of fault; Sense of slip: RL: Right lateral, LL: Left lateral, TH: Thust, NR: Normal; Top, Bott. (km): top and bottom of fault; T_s : slip tendency.

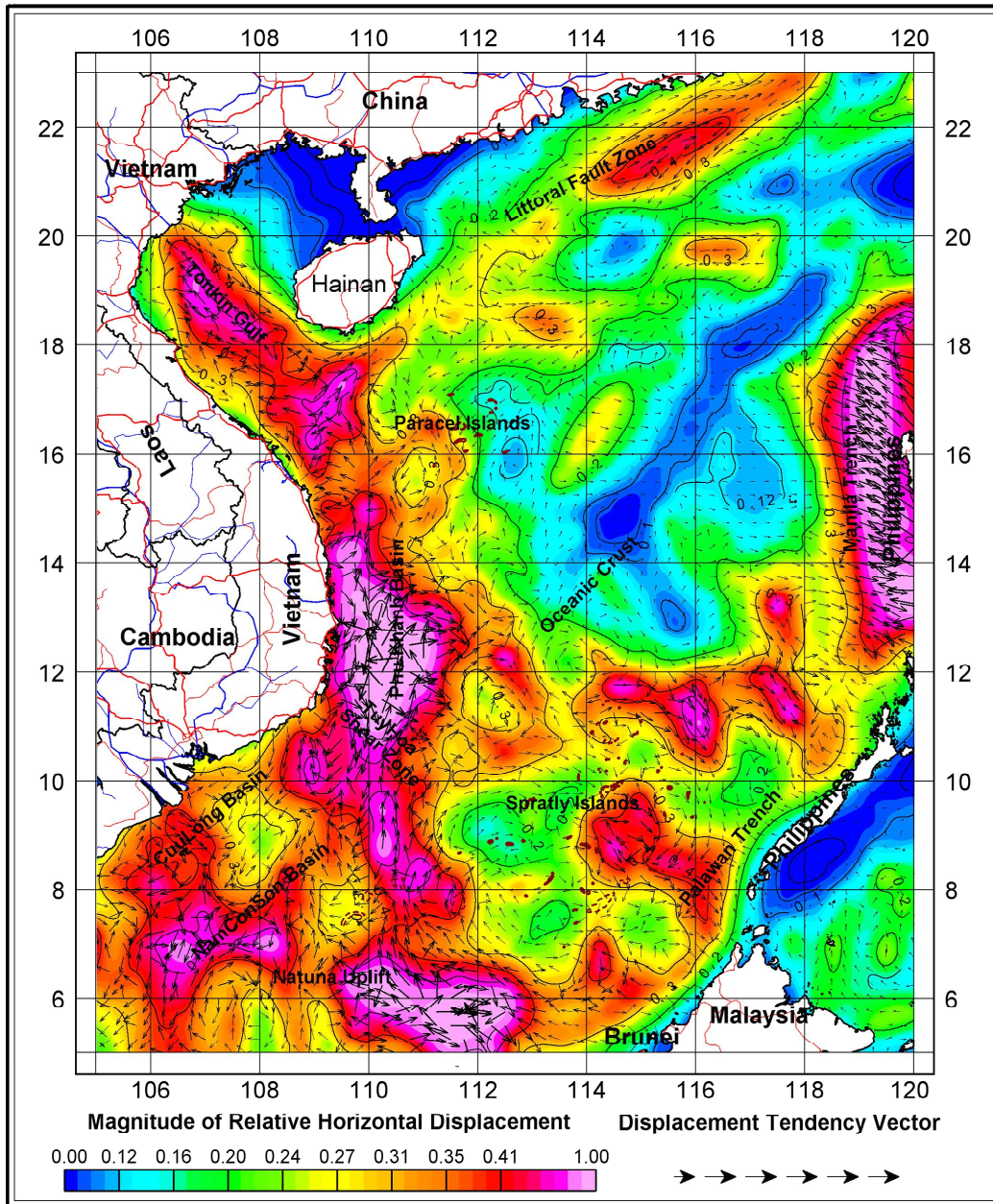


Fig. 8. Tendency and magnitude of relative horizontal displacement of the Earth's crust (determined by fault's parameters).

the RVD in the Manila trench area are quite high. It shows again the strong activity of the thrust faults in this area.

In the south of the study area, Natuna uplift, the tendency of the RVD is up, and its magnitude is greater than that around. In the deep water basin of the South China Sea, the magnitude of relative vertical displacement has an average value. It also has an interleaving of tendency up-down.

CONCLUSION

In the South China Sea and adjacent areas, the present-day regional stress field is determined through

the earthquake's focal mechanism parameters that have recorded more than 100 years. The geometric parameters of the faults are determined by gravity, seismic data and the above-mentioned regional stress fields.

The tendency and magnitude of relative displacement of the Earth's crust are calculated based on the relationship between the regional stress field with the fault geometric parameters. On the basis of these tendency and magnitude, the geotectonic mechanism can be rebuilt through different geological periods in the South China Sea and adjacent areas.

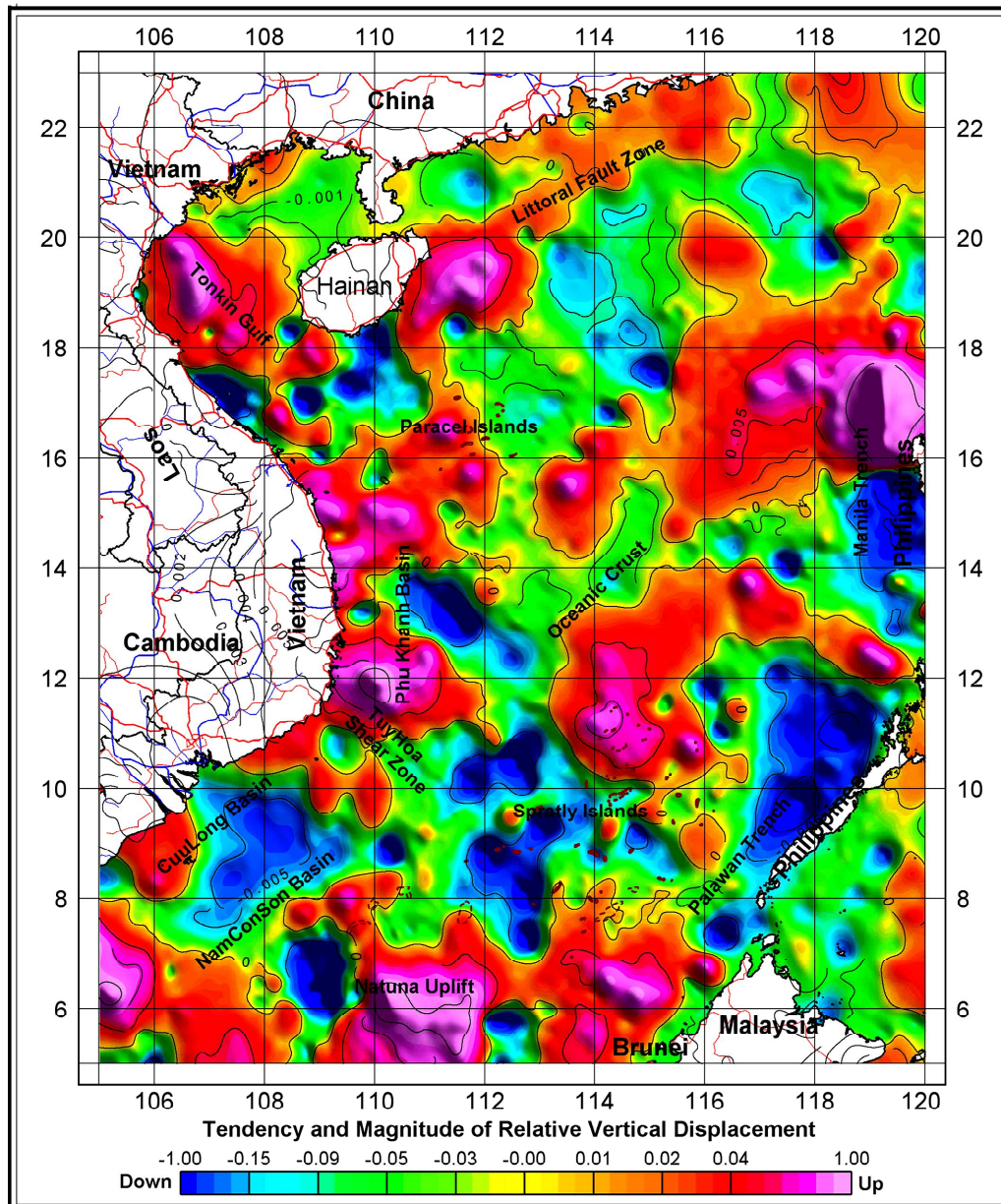


Fig. 9. Tendency and magnitude of relative vertical displacement of the Earth's crust (determined by fault parameters).

The present-day tectonic stress field plays a very important role in the slip activity of existent faults systems. The large fault systems, which have a high frictional coefficient, can accumulate more energy under the impact of stress field. To a sometime, when they have sufficient energy, they can react, break the geological structure and may cause the earthquake. This relationship can be seen as a key element in research of the risk of landslide, earthquake, tsunami.

ACKNOWLEDGMENTS

The authors wish to thank the VAST's Project No. VAST06.06/16-17 for funding this research.

REFERENCES

1. Aki K. and Richards P.G., 1980. Quantitative Seismology, Theory and Methods, Vol. I and II, W.H. Freeman, San Francisco.
2. Angelier J., 1990. Inversion of field data in fault tectonics to obtain the regional stress. III – A new rapid direct inversion method by analytical means, *Geophys. J. Int.*, Vol. 103, pp. 363–376.
3. Bott, M.H.P., 1959, The mechanisms of oblique slip faulting: *Geological Magazine*, Vol. 96, pp. 109–117.
4. Bui Cong Que et al., 2010. Hazard of earthquake and tsunami in Vietnam coastal zone. Science and technique publishing house, Hanoi. 320 pp.
5. <http://www.globalcmt.org/>

6. Karoly I. K., 1990, Transfer properties of the reduction of magnetic anomalies to the pole and to the equator. *Geophysics*, vol. 55, no. 9, 1141–1147.
7. McFarland J.M., Morris A.P., Ferrill D.A., 2012. Stress inversion using slip tendency, *Computers & Geosciences* 41, pp. 40–46.
8. McKenzie, D. P., 1969. The relation between fault plane solutions for earthquakes and the directions of the principal stresses, *Bull. seismol. Soc. Am.*, Vol. 59, pp. 591–601.
9. Morris, A., D. A. Ferrill, and D. B. Henderson (1996), Slip tendency analysis and fault reactivation, *Geology*, 24, 275–278.
10. Nguyen Van Vuong et al., Zoning and forecasting the present-day Earth's crust displacement in the Vietnam Northwest area on the basis of the research interaction between regional stress field with some fault systems. *Journal of Geology, series A*, 2004.
11. Okada Y., 1992. Internal deformation due to shear and tensile faults in half-space, *Bull. of the Seism. Soc. of America*, Vol. 82, No. 2, pp. 1018–1040.
12. Sandwell D. T., Garcia E., Soofi K., Wessel P., and Smith W. H. F., 2013, Towards 1 mGal Global Marine Gravity from CryoSat-2, Envisat, and Jason-1, *The Leading Edge*, 32(8), 892–899. doi: 10.1190/tle32080892.1.
13. Schellart W.P., 2000. Shear test results for cohesion and friction coefficients for different granular materials: scaling implications for their usage in analogue modeling, *Tectonophysics*, Vol. 324, pp. 1–16.
14. Toda S., Stein R. S., Richards-Dinger K. and Bozkurt S., 2005. Forecasting the evolution of seismicity in southern California: Animations built on earthquake stress transfer, *Journal of Geophysical Research*, Vol. 110, B05S16, doi:10.1029/2004JB003415.
15. Tran Tuan Dung et al. 2012–2015. Studying and warning the submarine landslide hazard in the Vietnam South central continental shelf. National Project, No. KC.09.11/11–15.
16. Tran Tuan Dung, Bui Cong Que, Nguyen Hong Phuong, 2013. Cenozoic basement structure of the South China Sea and adjacent areas by modeling and interpreting gravity data. *Russian Journal of Pacific Geology*. ISSN 1819–7140. Vol. 4. Pp. 227–236.
17. Tran Tuan Dung, Bui Cong Que, Nguyen Quang Minh, 2016. Distribution of eruptive volcanic basalt in the South China Sea and adjacent areas by interpreting gravity, magnetic and seismic data. *Russian Journal of Pacific Geology*. ISSN 1819–7140, 10(1), 1–12. DOI 10.1134/S1819714016010024.
18. Yukutake Y., Takeda T., Yoshida A., 2015. The applicability of frictional reactivation theory to active faults in Japan based on slip tendency analysis, *Earth and Planetary Science Letters* 411, pp. 188–198.
19. Schellart W.P., 2000. Shear test results for cohesion and friction coefficients for different granular materials: scaling implications for their usage in analogue modeling, *Tectonophysics*, Vol. 324, pp. 1–16.
20. Steketee J. A., 1958. On Volterra's dislocation in a semi-infinite elastic medium, *Can. J. Phys.*, Vol. 36, pp. 192–205.

Рекомендована к печати Р.Г. Кулиничем

Т. Туан Зунг, Буй Конг Цюэ, Нгуен Куанг Минь

Отношения между современным региональным полем напряжения и геометрическими параметрами разломов при определении относительного смещения земной коры в Южно-Китайском море и прилегающих районах

В статье определяется современное региональное поле напряжений в Южно-Китайском море с помощью фокальных параметров определения механизма землетрясений, установленных более 100 лет назад. Геометрические параметры разломов (такие как расположение, угол падения, угол простиранья, а также глубина, длина и горизонтальная деструктивная зона и т.д.) определялись по гравитационным, сейсмическим данным и региональным полям напряжения. Прогнозирование магнитуды и тенденции относительного смещения земной коры выполнены при вычислении и оценки взаимоотношений между региональными полями напряжений и геометрическими параметрами разломов. На основе относительного смещения земной коры можно реконструировать механизм геодинамических характеристик в различные геологические периоды в Южно-Китайском море и прилегающих территориях. Магнитуда и тенденция относительного смещения земной коры представлены в цветовом спектре и значениями вектора. Несмотря на то что смещение земной коры проявляется во всем регионе, существуют различия в интенсивности в отдельных районах с разнопорядковыми системами разломов.

Ключевые слова: разломы, современное региональное поле напряжений, смещение земной коры, Южно-Китайское море.